

Effective Molarity in Diffusion-Controlled Reactions

Michael H. Mazor, Chung F. Wong, J. Andrew McCammon,*

Department of Chemistry, University of Houston, Houston, Texas 77204-5641

John M. Deutch,*

Department of Chemistry, Massachusetts Institute of Technology, Cambridge, Massachusetts 02139

and George Whitesides*

Department of Chemistry, Harvard University, Cambridge, Massachusetts 02138 (Received: August 3, 1989; In Final Form: October 27, 1989)

Effective molarities for diffusion-controlled reactions between spherical reactants with reactive patches are calculated analytically and by Brownian dynamics simulations. Unimolecular reaction systems with internal translational motion in one, two, and three dimensions are investigated and compared with bimolecular reactions in three dimensions. Rotational diffusion is included in all cases in which a reactant particle is anisotropically reactive. Effective molarities are established by calculating the ratio $k_{\text{uni}}/k_{\text{bi}}$. Large rate enhancements are seen when restrictive translational constraints are imposed on the unimolecular reaction. Additional rate enhancements occur when a reduction in dimensionality accompanies the translational constraint. If the reactants are anisotropically reactive, the effective molarity is further increased if the geometric constraints in the unimolecular system keep the reactive surfaces in a proper orientation for reaction. The presence of an attractive potential designed to represent the relief of strain in the unimolecular system also leads to rate enhancements. The results are compared with those obtained for simple models of activated (non-diffusion-controlled) reactions. Overall, these simulation results indicate that highly elevated values of effective molarity are not likely to arise from mass transport considerations alone.

Introduction

In many chemical systems, a rate enhancement is seen when an intramolecular reaction replaces its intermolecular analogue, that is, when the two reactive species are part of the same molecule rather than separate molecules or atoms. Of course, any such comparison between different reactions assumes that the two reactions proceed through the same transition state. A quantity has been defined to measure this rate enhancement, namely, the effective molarity (EM). This is defined as the ratio of the intramolecular rate constant to the intermolecular rate constant.^{1,2}

Consider the rate equation for an elementary bimolecular reaction:



The relative rate of disappearance of A is

$$\frac{-d[A]}{dt} \frac{1}{[A]} = k_{\text{bi}}[B] \quad (2)$$

In the elementary unimolecular reaction



the relative rate of disappearance of A is

$$\frac{-d[A]}{dt} \frac{1}{[A]} = k_{\text{uni}} \quad (4)$$

The concentration of reactant B necessary for the two relative rates to be equal

$$k_{\text{bi}}[B] = k_{\text{uni}} \quad (5)$$

is the effective molarity of the unimolecular reaction:

$$[B] = k_{\text{uni}}/k_{\text{bi}} \equiv \text{EM} \quad (6)$$

The range of effective molarities seen in experiments extends from less than 1 M to greater than 10^8 M.² A number of theoretical models have been advanced to rationalize the observed EMs.³ Different theories have attributed high effective molarities

to proximity, steric, or strain effects. Depending on the theory and the particular system under study, maximum rate enhancements ranging from 5 M to greater than 10^8 M have been predicted.²⁻⁵

In the present work, we explore the variation in EM obtained for simple theoretical models in which both the intermolecular and intramolecular reactions are diffusion controlled. In these models, the reactants are spherical particles that are allowed to diffuse in either an unbounded or a bounded region of space so as to simulate a bimolecular reaction or a unimolecular reaction, respectively. The particles have reactive patches on their surfaces. A collision between the diffusing particles results in a reaction if the two reactive surfaces come into contact; otherwise, the particles reflect and diffuse apart. The model systems are chosen to allow us to explore how variations in the flexibility of the linking group influence the intramolecular reaction rate and corresponding effective molarity. The contribution to the effective molarity due to rotational mobility is also studied. Finally, the effects of an attractive potential intended to represent steric effects in the unimolecular system are also investigated.

One major objective of the work is to inquire if (or under what circumstances) very large values of EM can be attributed entirely to proximity (that is, to a favorable configurational entropy reflecting the restriction in relative position and orientation of the reactants in space to regions favoring reaction) and to what extent enthalpic terms must be considered. Restricting the treatment to diffusion-controlled reactions does not limit its scope in considerations of entropy. Thus this treatment provides an accurate (within the limits of the analysis) discussion of the maximum contribution to EM from proximity. Its conclusion—that proximity alone cannot account for values of EM larger than approximately 10^3 – 10^4 M—is not an artifact of a treatment considering only diffusion-controlled reactions.

Theory

Model System. The reactant particles in this work are spheres of 1-Å diameter. This size was chosen arbitrarily, with appropriate

(1) Mandolini, L. *Adv. Phys. Org. Chem.* **1986**, *22*, 1.

(2) Kirby, A. J. *Adv. Phys. Org. Chem.* **1980**, *17*, 183.

(3) Menger, F. M. *Acc. Chem. Res.* **1985**, *18*, 128.

(4) Dafforn, A.; Koshland, D. E. *Proc. Natl. Acad. Sci. U.S.A.* **1971**, *68*, 2463.

(5) Bruice, T. C.; Pandit, U. K. *J. Am. Chem. Soc.* **1960**, *82*, 5858.

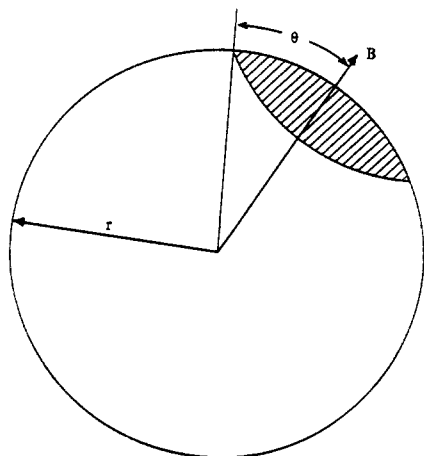


Figure 1. Model of reactive spheres of radius r with reactive patch angle of θ around the symmetry axis vector **B**.

scaling, the results presented here are generally applicable. The spheres can either be uniformly reactive or can possess an axially symmetric reactive zone. The angular size of the reactive patch measured from its axis of symmetry is denoted by θ (see Figure 1). The two reaction partners diffuse in a liquid with the viscosity of water at 300 K. There are no forces of interaction between the reactive particles in most of the calculations. In one calculation, a harmonic interparticle potential is used to model the relief of strain upon reaction in a unimolecular system.² In all calculations, hydrodynamic interactions are ignored.

The bimolecular reaction



occurs instantly when the two particles, diffusing in an infinite domain, collide on their reactive surfaces at a center-to-center separation $a = 1 \text{ \AA}$. The unimolecular reaction



is identical with the bimolecular reaction except that the two spheres are connected by a flexible chain or tether. There is therefore a maximum center-to-center separation R , which we take to be 10 \AA in most of these discussions (changes in the length of the tether are treated explicitly in the last section of the paper).

Three different types of molecular connectors will be considered for the unimolecular case. The most flexible connector allows the reactive spheres to move freely relative to each other in three dimensions. Two less flexible connectors allow relative motion in only two or one dimension; these connectors are idealized models for molecules in which reactive groups are attached to semirigid frames.

Calculating k_{bi} . Northrup et al. have developed and extended a method for calculating the rate of a bimolecular diffusion-controlled reaction via Brownian dynamics trajectory simulations.^{6,7} The simulation is performed in a bounded domain and then corrected for the infinite domain of the physical system. The formalism of Northrup et al. is general and can account for interparticle forces and for hydrodynamic interactions, although the latter are not included in the numerical evaluations of EMs in the present work.

The model system for the bimolecular reaction is one in which one member of the reacting pair (A) is centered at the origin and the other (B) is allowed to diffuse with a relative diffusion constant equal to the sum of the individual diffusion constants:

$$D_{rel} = D_A + D_B \quad (9)$$

We use a treatment based on the following simple model. The

space around A is divided into two regions. For values of the interparticle center-to-center separation $r > b$, we assume that the interparticle potential $u(r) = 0$. Thus, the rate constant for diffusing B particles to arrive at $r = b$ is given by a simple analytic expression (see below). The subsequent fates of B particles that have reached $r = b$ is determined by Brownian dynamics trajectory calculations. This allows for the computation of reaction probabilities when the geometric requirements for reaction do not admit analytic calculation. Any trajectory is terminated either by reaction (when B collides with A at $r = a$ and the reactive patches of A and B are properly oriented for reaction) or by truncation (when the B particle moves to a distance $r = q$, where $q > b$). As is described below in greater detail, the overall bimolecular rate constant k_{bi} is a simple function of the rate constant $k_D(b)$ for arrival at $r = b$, the probability $\hat{\beta}$ of subsequent reaction rather than truncation, and a factor Ω that corrects for the fact that the truncated trajectories, had they been continued, might have led to reaction rather than escape of the reactants to infinite separation.

The basic relation used to calculate k_{bi} is^{6,7}

$$k_{bi} = k_D(b)p \quad (10)$$

Here, $k_D(b)$ is the rate constant for the bimolecular reaction between the diffusing particle and an isotropically reactive target of radius b . This rate constant is given by the Smoluchowski expression⁸

$$k_D(b) = 4\pi D_{rel}b \quad (11)$$

The quantity p is the probability that a particle that starts at b will eventually react rather than diffuse to infinite separation. This quantity is calculated indirectly by carrying out Brownian dynamics simulations of reactant B in a finite region around the target A. A truncation sphere is established beyond b at $r = q$. When a particle reaches q its trajectory is terminated. The probability that a particle that starts at b will react rather than diffuse to $r = q$ is termed $\hat{\beta}$. In our calculations, b and q are taken to be 4 and 10 \AA , respectively. The probability p can be expressed in terms of the computed probability $\hat{\beta}$ by⁶

$$p = \hat{\beta} / (1 - (1 - \hat{\beta})\Omega) \quad (12)$$

The quantity Ω is the probability that a particle at q in an infinite domain will return to $r = b$ rather than diffuse to infinite separation. It can be expressed analytically as⁹

$$\Omega = k_D(b) \int_q^\infty dr \left\{ \frac{\exp[u(r)/k_B T]}{4\pi r^2 D(r)} \right\} \quad (13)$$

which for systems without interparticle forces ($u(r) = 0$) integrates to

$$\Omega = b/q \quad (14)$$

In summary, the rate constant for bimolecular reactions of particles with perfectly reactive patches but that have no interparticle or hydrodynamic interactions is⁶

$$k_{bi} = \frac{4\pi D_{rel}b\hat{\beta}}{1 - (1 - \hat{\beta})\Omega} \quad (15)$$

$\hat{\beta}$ is calculated by determining the ensemble probability that a particle starting at a random point on surface b (4 \AA) will react with a second particle anchored at the origin rather than diffuse to surface q (10 \AA).

Calculating k_{uni} . General Systems, via Computer Simulation. The rate constant for a unimolecular reaction is the reciprocal of the average reaction time (or mean first passage time) τ .¹⁰⁻¹²

(6) Northrup, S. H.; Allison, S. A.; McCammon, J. A. *J. Chem. Phys.* **1984**, *80*, 1517.

(7) Allison, S. A.; Northrup, S. H.; McCammon, J. A. *J. Chem. Phys.* **1985**, *83*, 2849.

(8) Smoluchowski, M. V. *Phys. Z.* **1916**, *17*, 557.

(9) Northrup, S. H.; Hynes, J. T. *J. Chem. Phys.* **1979**, *71*, 871.

(10) Szabo, A.; Schulten, K.; Schulten, Z. *J. Chem. Phys.* **1980**, *72*, 4350.

(11) Weiss, G. H. *Adv. Chem. Phys.* **1967**, *13*, 1.

In our model, τ will be calculated in the various unimolecular systems discussed above by determining the ensemble average time necessary for a particle starting at a random point within the diffusion region (all points greater than 1 Å from the origin and less than 10 Å from the origin) to react with a particle located at the origin. All attempts to diffuse to a separation greater than 10 Å are reflected back into the diffusing region to continue the trajectory until reaction occurs.

Isotropically Reactive Spheres, via Analytical Formulation. For the case of uniformly reactive spheres, the unimolecular diffusion-controlled reaction rate can be obtained analytically as the inverse of a mean first passage time. These times have been obtained by Adam and Delbruck using series solutions,¹² in closed form by Szabo et al. using operator methods,¹⁰ and by Deutch using direct integration.¹³ Here, we give a straightforward derivation using Laplace transforms.

The rate of change of the distribution function of the trapped particle, $P(r,t)$, can be expressed in terms of the diffusion equation

$$\partial P(r,t)/\partial t = D\nabla \cdot [\nabla P(r,t) + \beta(\nabla u(r))P(r,t)] \quad (16)$$

where D is the diffusion constant, $u(r)$ is the potential felt by the particle, and β is the reciprocal of the product of Boltzmann's constant and absolute temperature. The boundary condition at the reflective surface R is

$$-D[\nabla P(r,t) + \beta(\nabla u(r))P(r,t)]_{r=R} = 0 \quad (17)$$

This is equivalent to the particle flux at R being zero. The boundary condition at the reactive surface a is

$$P(r,t)_{r=a} = 0 \quad (18)$$

The initial distribution $P(r,t=0)$ is V^{-1} , where V is the volume of the system.

The diffusion equation is simplified by taking the Laplace transform

$$z\hat{P}(r,z) - V^{-1} = D\nabla \cdot [\nabla \hat{P}(r,z) + \beta(\nabla u(r))\hat{P}(r,z)] \quad (19)$$

where

$$\hat{P}(r,z) = \int_0^\infty e^{-zt} P(r,t) dt$$

The mean first passage time τ can be expressed as

$$\tau = \int_0^\infty dt \int dr P(r,t) = \int dr \hat{P}(r,z)|_{z=0} \quad (20)$$

where the integration over time is included in the Laplace transform of $P(r,t)$ with $z = 0$.

Inserting $P(r,z=0)$ into eq 19 yields

$$\frac{-1}{VD} = \frac{1}{r^{d-1}} \frac{d}{dr} r^{d-1} \left[\frac{d}{dr} \hat{P}(r,z=0) + \beta \left(\frac{d}{dr} u(r) \right) \hat{P}(r,z=0) \right] \quad (21)$$

where d is the dimensionality of the system.

Integration and application of the boundary condition at R yield

$$\frac{d\hat{P}(r,z=0)}{dr} + \beta \left(\frac{d}{dr} u(r) \right) \hat{P}(r,z=0) = \frac{1}{dVD} \left[\frac{R^d}{r^{d-1}} - r \right] \quad (22)$$

The left-hand side of eq 22 is equal to

$$e^{-\beta u(r)} \frac{d}{dr} e^{\beta u(r)} \hat{P}(r,z=0)$$

A second integration yields

$$\hat{P}(r,z=0) = \frac{1}{dVD} e^{-\beta u(r)} \int_a^r dx e^{\beta u(x)} \left[\frac{R^d}{x^{d-1}} - x \right] \quad (23)$$

Application of eq 20 gives a general expression for the mean first passage time:

$$\tau_d = \frac{A_d}{dVD} \int_a^R dr r^{d-1} e^{-\beta u(r)} \int_a^r dx e^{\beta u(x)} \left[\frac{R^d}{x^{d-1}} - x \right] \quad (24)$$

where $A_1 = 1$, $A_2 = 2\pi$, and $A_3 = 4\pi$.

When $u(r) = 0$, eq 24 can be integrated analytically. Expressions for the mean first passage times with no interparticle forces are given in eqs 25–27, where $\gamma = R/a$.

$$d = 1 \quad \tau_1 = \frac{a^2[\gamma - 1]^2}{3D} \quad (25)$$

$$d = 2 \quad \tau_2 = \frac{a^2}{2D(\gamma^2 - 1)} \left[\gamma^2 \ln \gamma - \frac{3}{4}\gamma^2 + 1 - \frac{1}{4\gamma^2} \right] \quad (26)$$

$$d = 3 \quad \tau_3 = \frac{a^2}{D} \left[\frac{5\gamma^6 - 9\gamma^5 + 5\gamma^3 - 1}{15(\gamma^3 - 1)} \right] \quad (27)$$

Computational Methods

Brownian Dynamics. Translational Motion. The stochastic translational motion of the diffusing particle is simulated by using the algorithm of Ermak and McCammon.¹⁴ The displacement of the particle along each Cartesian axis is given by an equation of the form

$$x(t + \Delta t) = x(t) + S \quad (28)$$

where Δt is the dynamics time step. S is a Gaussian random number with a mean of zero and a variance

$$\langle S^2 \rangle = 2D_{\text{rel}}\Delta t \quad (29)$$

which mathematically represents the stochastic forces imparted to the particle by the solvent. The random numbers S are generated for the simulation by the IMSL Library GGNML subroutine.¹⁵ As stated above, the relative diffusion constant is the sum of the individual diffusion constants, which can be calculated by the Stokes–Einstein law of diffusion:

$$D_i = \frac{k_B T}{6\pi\eta(a/2)} \quad (30)$$

The absolute temperature, T , is 300 K and the solvent viscosity, η , is 1 cP. The particle diameter, a , is 1 Å for both the target and the diffusing particle. The time step, Δt , is 5.69 fs and was arrived at through system parameters:

$$\Delta t = \frac{1}{100} \frac{(a/2)^2}{2D_{\text{rel}}} \quad (31)$$

It represents one-hundredth of the time step necessary for the variance of S to be the square of the particle radius.

Rotational Diffusion. The equation of motion for the direction vector representing the axis of symmetry of the reactive patch is

$$\mathbf{B}(t + \Delta t^R) = \mathbf{B}(t) \cdot \mathbf{M}_x \cdot \mathbf{M}_y \cdot \mathbf{M}_z \quad (32)$$

where \mathbf{M}_x , \mathbf{M}_y , and \mathbf{M}_z are rotation matrices corresponding to rotation around the x , y , and z axes by random angles α_1 , α_2 , and α_3 . The average of α_i is zero and the variance is

$$\langle \alpha_i^2 \rangle = 2\Delta^R \Delta t^R \quad (33)$$

where D^R is the Stokes' law rotational diffusion constant

$$D^R = \frac{k_B T}{8\pi\eta(a/2)^3} \quad (34)$$

The random numbers α_i are generated by the IMSL Library GGNML.¹⁵ The time step for rotation, Δt^R , is 10 times as large as Δt , the time step for translation, but rotations are performed

(12) Adam, G.; Delbruck, M. *Structural Chemistry and Molecular Biology*; Rich, A., Davidson, N., Eds.; Freeman: San Francisco, 1968; pp 198–215.

(13) Deutch, J. M. *J. Chem. Phys.* **1980**, *78*, 4700.

(14) Ermak, D. L.; McCammon, J. A. *J. Chem. Phys.* **1978**, *69*, 1352.

(15) IMSL Library Edition 9.2 (IMSL LIB-0009, Houston, TX 1984).

once every 10 translational steps.

Time-Step Variation. To save computation time, the time step, and thus the variance of the random number in the equation of motion, was varied according to the position of the diffusing particle relative to the target. In the bimolecular system with a reactive surface at a ($r = 1 \text{ \AA}$) and a truncation surface at q ($r = 10 \text{ \AA}$), the intervening region was divided into seven shells of equal width. The two zones closest to the target had time-step values as stated above, the third zone had a time step 10 times larger, and the remaining four zones had time steps 20 times larger than the minimum value. In all cases the rotational time step was 10 times the translational time step. The trajectory initiation surface b ($r = 4 \text{ \AA}$) was inside of the third zone.

In the unimolecular system, the region between the reaction surface at a ($r = 1 \text{ \AA}$) and the reflective surface ($r = 10 \text{ \AA}$) was also divided into seven regions, with the regional time steps symmetric about zone 4. Zones 1 and 7 had the minimum time step as calculated above, and zones 2 and 6 had time steps 10 times larger. The time steps for zones 3 and 5 were 25 times larger than the minimum, and that for zone 4 was 50 times larger than the minimum.

These particular time-step distributions were experimentally arrived at so as to reproduce the results of a uniform time-step distribution corresponding to the minimum value throughout the interval. The values used in all cases were derived from the three-dimensional systems that were the most sensitive to the time-step distribution.

Boundary Conditions. Starting Positions. In the calculation of the bimolecular rate constant, the diffusing particle was started at random locations on the surface b (4 \AA). The simulation used the IMSL Library GSPH¹⁵ subroutine for this purpose.

In the calculation of the unimolecular rate constant, the diffusing particle was started at random locations in the diffusion region by using IMSL Library GGUBFS.¹⁵ This results in an ensemble average uniform distribution of starting positions, as required in calculations of mean first passage times.¹⁰

Reaction. In both the unimolecular and bimolecular models, reaction occurs on contact between the reactive portions of the particles. Computationally, three criteria must be met. First, the center-to-center displacement must be less than or equal to the sum of the radii of the particles. If the target is anisotropically reactive, a puncture point is calculated. This point is defined as the point on the target surface that the diffusing molecule would have passed through if a straight line between the last point on the trajectory and the present point were assumed. The second requirement for reaction is that the angle of the puncture point relative to the symmetry axis of the target must be less than or equal to θ , the angle that defines the target's reactive patch. The third criterion is evaluated if the diffusing particle has anisotropic reactivity. The line from the center of the target to the center of the diffusing molecule, if it were touching at the puncture point, is calculated; the angle between this line and the symmetry axis of the diffusing particle's reactive patch must be less than or equal to the angle θ_2 that defines the reactive patch on the diffusing particle.

When the conditions for reaction are achieved in the bimolecular case, the counters corresponding to the number of reactions and the number of runs (NRXN and NRUN, respectively) are both incremented by 1. The probability β is calculated as NRXN/NRUN when NRUN is equal to 4000.

In the unimolecular simulations, the reaction time t_{rxn} for a given run is $t + \Delta t$, where t was the lifetime of the reactants on the last step prior to reaction. The mean first passage time is then simply the ensemble average of the reaction times.

Reflection. In the calculation of the probability β in the bimolecular simulation, the diffusing molecule may attempt a step through a reflective boundary on the anisotropic particle. If this occurs, the position at $t + \Delta t$ is equated with the position at t and a new Brownian step is performed. The unimolecular model treats reflection in a similar manner, both for collisions of the reactants and for displacements of the reactants beyond the allowed maximum (10 \AA). The position at $t + \Delta t$ is equated with the position

TABLE I: Effective Molarities (M) for Different Combinations of Unimolecular Reactions (Columns) and Bimolecular Reactions (Rows)^{a,b}

bimolecular reactions	unimolecular reactions						
	1D	2D	3D	3D ^c 90:180	3D 45:180	3D 30:180	3D 30:30
3D	5.17	1.63	0.470				
3D				0.448			
90:180	6.85	2.16	0.623				
3D				0.904	0.402		
45:180	13.82	4.36	1.26				
3D				1.49	0.664	0.411	
30:180	22.81	7.19	2.08				
3D				13.6	6.06	3.76	0.356
30:30	208.1	65.62	18.9				

^aThese results are based on computer simulations. The reaction distance $a = 1 \text{ \AA}$ and the reflection distance $R = 10 \text{ \AA}$ in all cases. ^bThe uncertainties range from 4% to 10% with the average being 6%. These are obtained by propagating the standard deviation of the mean unimolecular and bimolecular rate constants from eight batches of 500 trajectories each. ^cReactive patch on target (θ in degrees):reactive patch on diffusing particle (θ_2 in degrees).

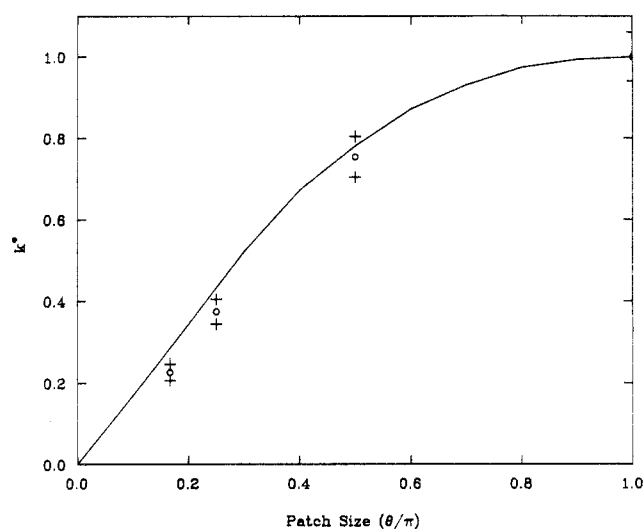


Figure 2. Effect of target reactive patch size θ on bimolecular rate constant. k^* is the bimolecular rate constant divided by the Smoluchowski result ($4\pi D_{\text{rel}} a$), where a is the sum of the radii. The solid line corresponds to the analytical results of Shoup et al.¹⁶ Points correspond to the simulation results. Crosses correspond to the error range obtained by propagating the standard deviation of the mean bimolecular rate constants from eight batches of 500 trajectories each.

at t , Δt is added to the lifetime of the reactant, and the Brownian dynamics trajectory is resumed.

Truncation. In the bimolecular simulation, trajectories are truncated when the interparticle separation is greater than q (10 \AA). The value of NRUN is then incremented while the value for NRXN remains the same, and a new trajectory is started.

Results and Discussion

Unimolecular rate constants were calculated for one-, two- and three-dimensional systems in which both particles were isotropically reactive (that is, the reactive patch size is 360°). In addition, in the three-dimensional systems the target particle was assigned three different reactive patch sizes: 90, 45, and 30° . One additional case was investigated, that in which both the target and diffusing molecule had a 30° reactive patch. The same systems were also investigated in the bimolecular case, which allowed us to evaluate the effects of spatial constraint on each system. The results can be found in Table I.

Shoup and Szabo¹⁶ derived an approximate analytical expression for the rate constant of a bimolecular reaction when one of the

TABLE II: Effective Molarities (M) for Uniformly Reactive Spheres^a

reactant dims				EM			rel EM		
<i>a</i> ^b	<i>R</i> ^b	<i>R</i> - <i>a</i>	<i>R/a</i>	1D	2D	3D	1D/2D	1D/3D	2D/3D
0.5	2.5	2.0	5.0	198	90.3	38.8	2.19	5.10	2.32
0.5	1.25	0.75	2.5	1410	888	554	1.59	2.55	1.60
0.5	0.55	0.05	1.1	317000	302000	288000	1.05	1.10	1.05
1.0	10.0	9.0	10.1	4.89	1.67	0.482	2.92	10.1	3.47
1.0	2.5	1.5	2.5	176	111	69.2	1.59	2.55	1.60
1.0	1.25	0.25	1.25	6340	5670	5060	1.12	1.25	1.12
2.0	5.0	3.0	2.5	22.0	13.9	8.65	1.58	2.55	1.60
2.0	4.0	2.0	2.0	49.5	34.9	24.4	1.42	2.03	1.43
2.0	2.25	0.25	1.12	3170	2990	2820	1.06	1.12	1.06

^aThe bimolecular reactions are all in three dimensions, and the unimolecular reactions are in one, two, or three dimensions. These results are based on analytical formulas, i.e., the unimolecular rate constants (in units of s⁻¹) are reciprocals of the mean first passage times given in eqs 25-27, and the bimolecular rate constants are given by the familiar Smoluchowski equation⁸ (in units of M⁻¹ s⁻¹). ^b*a* = reaction distance (Å), *R* = reflection distance (Å).

species is anisotropically reactive. Comparing the rate constants for the bimolecular simulations with their results reveals close agreement (see Figure 2).

The effective molarity in systems where the unimolecular reaction is exactly the same as the bimolecular reaction except for the translational constraint is seen to be less than 1 for all cases (see Table I). This result indicates that proximity alone is not solely responsible for the rate enhancements seen in the unimolecular reactions.^{3,17}

The maximum effective molarity in the absence of interparticle potentials occurs when the three-dimensional bimolecular reaction is between particles with relatively small reactive regions, and the corresponding unimolecular reaction is between reactive groups that are pointed toward each other with all motion confined to the line separating the two groups.

When the reactive species are isotropically reactive, effective molarities can be calculated analytically. Using the formalism outlined above, the rate constants for the unimolecular reactions can be calculated. An interesting result that is immediately apparent is that, because *k*_{uni} and *k*_{bi} are both inversely proportional to the diffusion constant, the effective molarity is independent of the viscosity. The effective molarities calculated analytically are in good agreement with those obtained from the simulations (compare Table I row 1 with Table II row 4). Analytic effective molarities for a wider variety of isotropically reactive systems without interparticle forces are compared in Table II. In this table, *a* is the reaction distance and *R* is the reflection distance. In all cases, the bimolecular rate constant is the Smoluchowski result, *k*_{bi} = 4π*D*_{rel}*a* for diffusion in three dimensions.

Three general effects can be discerned from the data. First, as the value of *R* - *a* decreases, corresponding to restricting the reactive species to a smaller and smaller region, the effective molarity increases dramatically. Using the analytic formulas in eqs 25-27 one can obtain expressions for the limiting behavior of the effective molarity. For example, for the three-dimensional bimolecular reaction and one-dimensional unimolecular reaction, *k*_{uni} and the effective molarity approach infinity as (*R* - *a*)⁻² as *R* approaches *a*. Second, as the ratio *R/a* of the reflective distance to the reactive distance goes from ≫ 1 to ≅ 1, the increases seen in reducing the dimensionality of the unimolecular system drop markedly. In three dimensions, the diffusing particle is nearly restricted to the surface of the target particle when *R/a* ≅ 1. In this case, the diffusing particle will react before it has been able to move an appreciable distance over this surface. The effective motion is essentially one-dimensional, which explains the convergence of the effective molarities for different dimensionalities of unimolecular motion as *R/a* → 1. Also of interest is the fact that the rate increase in reducing the dimensionality by 1 unit is similar regardless of whether one starts in three or two dimensions.

When an attractive interparticle potential is applied in the unimolecular case, the effective molarities increase dramatically,

TABLE III: Effective Molarities (M) for Uniformly Reactive Spheres with an Interparticle Potential in the Unimolecular Case of the Form^a

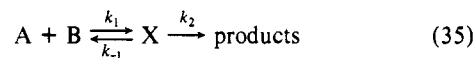
$$u(r) = f \left(\frac{r-a}{R-a} \right)^2$$

dimensionality ^b	effective molarity		
	<i>f</i> = 1.0	<i>f</i> = 1.0 × 10 ³	<i>f</i> = 1.0 × 10 ⁶
1	8.00	1460	9.34 × 10 ⁵
2	3.17	1280	9.18 × 10 ⁵
3	1.07	1180	9.14 × 10 ⁵

^aThe Smoluchowski result for the bimolecular case *k*_{bi} = 4π*Da* is used in all examples. These results are based on numerical integration of eq 24. *a* = 1.0 (Å), *R* = 10.0 (Å). Units of *f* are kcal·mol⁻¹. Integration was performed using the IMSL library DTWODQ.¹⁵
^bDimensionality of unimolecular reaction.

as seen in Table III. As the force constant *f* increases, the advantage of the unimolecular reactions of lower dimensionality is lost. This is due to the very strong potential forcing the particles to move straight toward each other regardless of the dimensionality of the space available for diffusion. The attractive potential here is intended to model the relief of strain in the case of reactants fused to a common molecular framework. Such relief of strain has long been thought to be an important factor in reactions that display large effective molarities,^{1,2} the present results support this view.

The results for diffusion-controlled reactions without interparticle forces can also be compared to results for models in which the reaction is activated rather than diffusion controlled but in which all other features are unchanged. Consider the reaction



and let *k*₁ ≫ *k*₂ so that the reaction is not diffusion controlled; rather, the rate is limited by the activated process corresponding to *k*₂. The usual steady-state analysis^{18,19} yields

$$k = Kk_2 \quad (36)$$

where *K* = *k*₁/*k*₋₁ is an equilibrium constant for the formation of the encounter complex X. If A and B are distinct molecules, the reaction is bimolecular and²⁰

$$K = K_{bi} = Lv \quad (37)$$

where *L* is Avogadro's number and *v* is the volume in liters available for relative translation of A and B in the encounter complex X. If, however, A and B are fragments of the same molecule, the reaction is unimolecular and²⁰

$$K = K_{uni} = v/V \quad (38)$$

(18) Calef, D. F.; Deutch, J. J. *Annu. Rev. Phys. Chem.* **1983**, *34*, 493.

(19) McCammon, J. A.; Northrup, S. H.; Allison, S. A. *J. Phys. Chem.* **1986**, *90*, 3901.

(20) McQuarrie, D. M. *Statistical Mechanics*; Harper & Row: New York, 1976.

(17) Menger, F. M.; Venkataram, U. V. *J. Am. Chem. Soc.* **1985**, *107*, 4706.

where v is as defined above and V is the volume in liters available for relative translation of A and B excluding the reactive volume v . Then the effective molarity is

$$EM = K_{\text{uni}}k_2/K_{\text{bi}}k_2 = (LV)^{-1} \quad (39)$$

For the three systems in the rows 4-6 of Table II, and 3D unimolecular reactions, the activated (diffusional) effective molarities are, respectively, 0.40 (0.48 M), 27 (69 M), and 416 M (5060 M). These three systems differ only in the volume V available for unimolecular fragment diffusion outside the reactive volume v ; the bimolecular reactions are the same for the three systems. The rate constant k_{uni} and the EM of the diffusion-controlled reactions increase more rapidly with decreasing V than do those of the activated reactions. This is due to the nonuniform distribution of reaction partners in the (nonequilibrium) diffusion-controlled reaction.

Conclusion

Simple diffusion-controlled reactions between spherical, isotropically reactive groups can display large rate enhancements when restrictive translational constraints are imposed on the

unimolecular reaction. Additional rate enhancements occur when a reduction in dimensionality accompanies the translational constraint unless the latter is very restrictive. If the reactants are not isotropically reactive, the effective molarity will be further increased if the geometric constraints in the unimolecular system keep the reactive surfaces in a proper orientation for reaction. Very large rate enhancements can occur when an attractive potential operates between the reactive groups in the unimolecular system, corresponding to some form of internal strain relief upon reaction.

These simulation results indicate that highly elevated values of effective molarity are not likely to arise from mass transport considerations alone. To reach effective molarities greater than about 10^3 , it is necessary to have favorable energetics, modeled here by an attractive intramolecular potential, or geometries so constrained that the concept of reactants separated by a tether becomes questionable.

Acknowledgment. This work has been supported in part by NIH, NSF, and the Robert A. Welch Foundation. M.H.M. is supported by an NIH Traineeship under the Houston Area Biophysics Training Program. J.A.M. is the recipient of the 1987 Hitchings Award from the Burroughs Wellcome Fund.

Electric Field Effect on the Chemical Activation Processes of 1,1,2,2-Tetrafluorocyclopropane

G. Arbilla, J. C. Ferrero,* and E. H. Staricco

INFIQC, Departamento de Físico Química, Facultad de Ciencias Químicas, Universidad Nacional de Córdoba, Sucursal 16, C. C. 61, 5016 Córdoba, Argentina (Received: July 31, 1989; In Final Form: October 13, 1989)

The electric field effect on the decomposition and energy-transfer process of chemically activated 1,1,2,2-tetrafluorocyclopropane is studied. The apparent unimolecular rate constant is measured as a function of the electric field strength in the range 0-7.2 kV/cm. A significant dependence of the experimental constant on the electric field was observed up to a saturation value. Several explanations for this behavior are analyzed.

Introduction

In recent years there has been great theoretical and experimental interest in the influence of electric and magnetic fields on transport properties,¹ energy absorption,² radiative and non-radiative processes,^{3,4} and reaction mechanism^{5,6} of gases, microemulsions,⁷⁻¹⁰ and crystals.^{6,11,12} Unfortunately, many questions remain unsolved, mainly those concerned with highly excited polyatomic systems. In previous papers¹³⁻¹⁵ we have studied the

decomposition and deactivation of highly vibrationally excited 1,1,2,2-tetrafluorocyclopropane. We now report the characterization of this process in a dc electric field. The data show a strong dependence of the unimolecular rate constants with the electric field strength. The results are discussed in terms of the current understanding of unimolecular processes.

Experimental Section

Reactants were obtained and purified as described previously.^{13,14} The samples were photolyzed with the unfiltered light of an OSRAM 500-W high-pressure mercury lamp, in cylindrical Pyrex vessels of diameter as small as possible compared with that of the electrodes. The diameter of the cell was typically 1-2 cm. In each experiment the cell was placed between two parallel circular plate electrodes made of polished aluminum, of 30 cm diameter, which were spaced 3 cm apart. The electrodes were connected to a HV power supply, which provided voltage in the range 0-30 kV, controlled to better than 5%. From the configuration used in this work, the dc electric field strength in the cell (E) can be related to the unperturbed field strength far from the Pyrex cell (E_0) by $E \sim 0.9E_0$. In calculating this relation, using a similar formulation to that of Gozel and van den Bergh,² it has

- (1) Beenakker, J. J. M.; Court, F. R. *Rev. Phys. Chem.* **1970**, *21*, 47.
- (2) Gozel, P.; van den Bergh, H. *J. Chem. Phys.* **1981**, *74*, 1724.
- (3) Stannard, P. R. *J. Chem. Phys.* **1978**, *68*, 3932.
- (4) Freed, K. F. *Adv. Chem. Phys.* **1981**, *47*, Part 2, 291.
- (5) Shulten, K. *J. Chem. Phys.* **1985**, *82*, 1312.
- (6) Weller, A.; Staerk H.; Treichel, R. *Faraday Discuss. Chem. Soc.* **1984**, *78*, 271.
- (7) Scaiano J. C.; Lougnot, D. *J. Chem. Phys. Lett.* **1984**, *105*, 535.
- (8) Scaiano J. C.; Lougnot, D. *J. Phys. Chem.* **1984**, *88*, 3379.
- (9) Tanimoto, Y.; Takashima M.; Itoh, M. *J. Phys. Chem.* **1984**, *88*, 6053.
- (10) Khudyakov, I. V.; Prokofiev, A. I.; Margulis L. A.; Kuzmin, V. A. *Chem. Phys. Lett.* **1984**, *104*, 409.
- (11) Patel J. S.; Hanson, D. M. *J. Chem. Phys.* **1981**, *75*, 5203.
- (12) Hanson, D. M. *Mol. Cryst. Liq. Cryst.* **1980**, *57*, 243.
- (13) Arbilla, G.; Ferrero, J. C.; Staricco, E. H. *J. Phys. Chem.* **1983**, *87*, 3906.
- (14) Arbilla, G.; Ferrero J. C.; Staricco, E. H. *J. Phys. Chem.* **1984**, *88*, 5221.

(15) Boaglio, D. G.; Arbilla, G.; Ferrero, J. C.; Staricco, E. H. *Int. J. Chem. Kinet.*, **1989**, *21*, 1003.